RSC Advances

PAPER

View Article Online
View Journal | View Issue

Cite this: *RSC Adv.*, 2021, **11**, 9568

Gold nanoparticles grafted with chemically incompatible ligands†

Joanna M. Wolska,* Aleksandra Błażejewska, Martyna Tupikowska, Damian Pociecha and Ewa Górecka

Received 21st January 2021
Accepted 22nd February 2021

DOI: 10.1039/d1ra00547b

rsc.li/rsc-advances

Janus-type structures were obtained from gold nanoparticles grafted with two types of chemically incompatible mesogenic ligands with a strong tendency for nano-segregation. A lamellar arrangement, in which metallic nanoparticle-rich sublayers are separated by organic ligand-rich sublayers of various composition, was formed due to the ligand segregation process. The layers could be easily aligned by mechanical shearing; for most materials the layer normal was parallel to the shearing direction but perpendicular to the shearing gradient, such transverse mode is only rarely observed for lamellar materials. Reversible changes of layer thickness under UV light were observed due to the presence of an azo-moiety in the organic ligand molecules.

Thin films made of nanoparticles (NPs) with a metallic core and organic shell are highly attractive materials with unusual optoelectronic and physicochemical properties 'encoded' in the inorganic and organic parts of the NPs.[1–5] Due to their wide application potential,[6–8] new, simple methods of assembling and controlling the structure of solid-state nanocomposites are intensively studied.[9,10] Controlling the shape of the inorganic parts is a critical factor on the way to accessing a wide variety of symmetries of structures made of NPs. However, methods to control the shape of the organic coating of NPs independently on the shape of the inorganic core could further broaden our capabilities to 'encode' properties of NPs thin films.[1,6,11] Janus particles are particular group of NPs that combine two dissimilar chemical or physical functionalities at their opposite sides.[12–15] Due to the geometrical asymmetry of Janus particles their self-assembling results in superstructures with hierarchical architecture of appreciable complexity and unusual properties.[16] The asymmetry of the particles can be obtained by merging two different inorganic core parts[17–20] or by functionalization of the particle surface with different organic modifiers.[21–24] The latter approach was used for example to obtain amphiphilic gold nanoparticles grafted with hydrophilic and hydrophobic ligands,[25,26] with two different polymers[27–29] or with triphenylphosphine and D-penicillamine.[30]

There is also a limited number of Janus particles obtained by grafting inorganic core with mesogenic ligands having amphiphilic properties built into single molecules.[31,32] However, obtaining the asymmetry in the grafting layer by synthetic method is not an easy task, therefore we decided to take different approach. The mesogenic ligands that are chemically dissimilar (having perfluorinated and alky chains) were attached to the metal surface on long flexible chains to ensure the flexibility of organic layer and enable rearrangement of the ligands around the metallic core. We assume that while in solution or isotropic state the ligands are homogenously distributed at the metal surface, upon lowering temperature chemically dissimilar ligands will start to self-segregate in space as it is often observed for liquid crystalline state – leading to formation of Janus type particles.

Herein we designed and obtained four mesogenic and promesogenic surface ligands for NPs grafting, that can be divided into two series based on their rigid mesogenic units and type of the terminal chain. All the ligands have a dimeric structure (Scheme 1), comprising two rigid parts: azobenzene and benzoiloxy (Series I) and biphenyl and *trans*-stilbene units

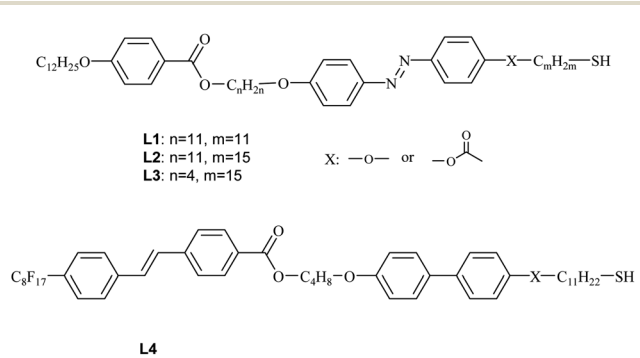

Scheme 1 Scheme of the building of Series I and II ligands.

Department of Chemistry, Warsaw University, Pasteura 1, 02-093 Warsaw, Poland. E-mail: jokos@chem.uw.edu.pl; Tel: +48 22 822 0211

† Electronic supplementary information (ESI) available: Synthesis, chemical characterization of obtained materials and detailed description of experimental methods used for structure studies. See DOI: 10.1039/d1ra00547b

(Series II). These rigid parts are connected by alkyl linkers, 4- or 11-carbon atom long. This dimeric structures ensure sufficient flexibility and softness of organic coating. The azobenzene unit additionally provide the ligands with light-responsive properties.

Molecules are terminated with 11- or 15-carbon atom chains, end-functionalized with a mercapto group to enable attachment to gold nanoparticles. The other terminal chain was either a hydrophobic dodecyloxy chains (Series I) or a perfluorinated hydrophilic chain (Series II). The structures of the obtained compounds were confirmed by spectroscopic methods (for more details see ESI†). Based on previous experiments[33,34] we expected these ligands would facilitate self-assembling of covered NPs into complex structures.

Liquid crystalline properties of obtained ligands were tested with polarizing microscopy (POM), formation of SmA phase by two compounds of Series I was confirmed (Table 1).

The spherical gold nanoparticles were obtained according to the Brust–Schiffrin method[35] using *n*-dodecanethiol to passivate the metallic surface. The primary coating of *n*-alkyl thiols improves the solubility of NPs and prevents their aggregation. The size of the metallic core, 2.4 ± 0.2 nm, was estimated from low angle X-ray scattering from particles dissolved in toluene.

The surface of the synthesized gold nanoparticles was modified by the functional ligands (L) synthesized as described above. Hybrid nanomaterials, H1–H4, comprising L1–L4 ligands, respectively were prepared. Additionally, amphiphilic hybrid nanoparticles H5, containing two types of secondary ligands were obtained; hydrophobic L3 and hydrophilic L4 ligands were attached in a 1 : 1 ratio, confirmed by TGA measurements[36] (for details see ESI†).

All the obtained hybrid materials were examined for their structural properties. In POM studies, shear-aligned samples of all hybrids showed optical birefringence (Fig. 1), however for nanoparticles H5 the birefringence was hardly detectable. Apparently, ligands attached to metallic cores show some orientational order for hybrids H1–H4 but remain in almost disordered state for H5 materials. Upon heating, all the materials undergo transition to isotropic liquid phase.

To reveal details of NPs arrangement in condensed state small-angle X-ray diffraction studies (SAXRD) were performed for thin film samples aligned by mechanical shearing. The XRD patterns obtained for all sheared samples comprised a series of commensurate signals along a common azimuthal direction (Fig. 2) and a broad signal along the orthogonal direction, such a pattern is characteristic of lamellar phase. According to our

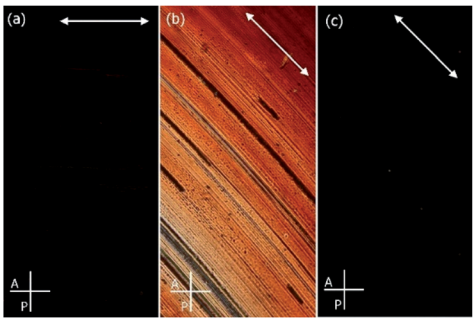

Fig. 1 Shear-aligned sample of H1 material at 40 °C observed between crossed polarizers P and A, with the shearing direction, marked with arrow, being along (a) and inclined (b) from the polarizer direction. (c) After melting the sample at 120 °C the birefringence is lost.

previous works formation of lamellar phases is driven by partial segregation of mesogenic and *n*-alkyl ligands on the NP surface in such a way that an overall shape of hybrid NP becomes anisotropic (cylindrical), that facilitate their packing into layers.[33,34,37,38]

Diffraction signal positions are collected in Table 2. The formation of a layered structure by hybrid nanoparticles is possible as the ligands being attached on flexible chains can easily move in space to achieve non-uniform distribution around nanoparticle core, *e.g.* they accumulate above and below the metallic core. As the determined layer thickness is much smaller than the diameter of a hybrid nanoparticle (twice the ligand length and diameter of the metallic core) it is obvious that ligands strongly intercalate between layers.

As evidenced by the POM and SAXRD studies, layers could easily be oriented by mechanical shearing. Interestingly, most of the materials align in a transverse mode in which the layer normal is parallel to the shearing direction but perpendicular to the shearing gradient; such an alignment mode was never observed for low weight LC molecules as stable configuration and only rarely for LC nanoparticles.[33] The only exception was material H2, with the longest ligand having a hydrophobic terminal chain, that aligned with perpendicular mode, *i.e.* with the layer normal perpendicular to both: the shearing direction and the shearing gradient.

The most interesting was the temperature evolution of the structure formed by H5 hybrid, in which the surfaces of

Table 1 Liquid crystal properties of ligands Series I (L1–L3) and Series II (L4)

No.	R	*n*	*m*	X	Properties
L1	$-OC_{12}H_{25}$	11	11	–O–	Iso 95 °C SmA 80 °C Cry
L2	$-OC_{12}H_{25}$	11	15	–OOC–	Iso 83 °C SmA 77 °C Cry
L3	$-OC_{12}H_{25}$	4	15	–OOC–	Iso 73 °C Cry
L4	$-C_8F_{17}$	4	11	–OOC–	Iso 200 °C Cry

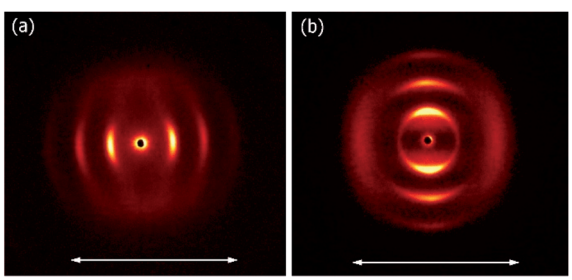

Fig. 2 SAXRD patterns for aligned samples of (a) H1 and (b) H2 materials, pointing to transverse and perpendicular alignment modes, respectively. Arrows show the shearing direction.

Table 2 Diffraction signal positions obtained for hybrids H1–H5. *D* is the estimated ligand molecule length

No.	XRD details	*D* (Å)
H1	79 Å, 40 Å, dyf: 40 Å	64.8
H2	81 Å, 40 Å, 28 Å, dyf: 35 Å	70.8
H3	72 Å, 38 Å, dyf: 35 Å	62.8
H4	85 Å, 40 Å, dyf: 31 Å	60
H5	T = 30–130 °C: 66 Å, dyf: 42 Å	62.8
	T = 140 °C: 135 Å, 65 Å dyf: 42 Å	60

nanoparticles were functionalized with a mixture of L3 and L4 ligands. Complex polymorphism for this material was confirmed by SAXRD measurements.

At room temperature, the distance between neighbouring layers was ~65 Å, pointing to an intercalated structure, similar to that observed for H1–H4. For the samples slowly heated to 150 °C signals corresponding to twice this periodicity (~145 Å) appear. Apparently, at higher temperatures, an annealing process takes place, in which the fluorinated and alkyl ligands start to nanosegregate and form separate sublayers (Fig. 3). In resulting Janus-type structure the metal-rich layer is surrounded by organic sublayers with different chemical composition: dodecyloxy chains rich or a perfluorinated chain rich. Moreover, if the sample is heated rapidly (with the heating rate above 2 K min^{-1}) to the temperature at which the annealing process takes place a different lamellar structure is formed, in which the basic periodicity is ~200 Å, almost 3 times larger than that observed for virgin samples. The structure with a repeating unit of three layers is probably due to only partial segregation of incompatible ligand molecules between sublayers of metallic cores (Fig. 3). After lowering the temperature, nanosegregation of incompatible building elements is preserved, either bi-layer or triple-layer structure is stable and does not change also in consecutive heating runs. Since the lamellar phase for H5 material is only weakly optically birefringent, one can assume that contrary to hybrids H1–H4, the ligands in the organic layer are not well orientationally ordered and remain in a nearly liquid state.

All hybrid materials can be melted to an isotropic liquid state, for which in XRD pattern only signal related to the average distance between particles is observed. The melting

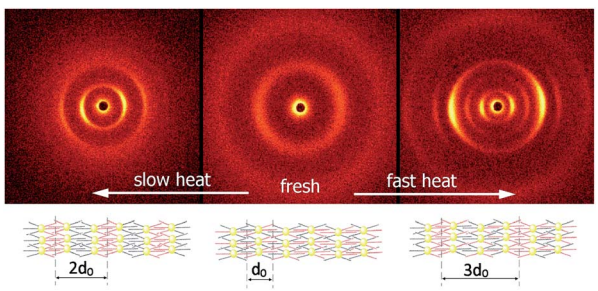

Fig. 3 2D SAXRD patterns of fresh and annealed samples of H5 material and model of structures with single, double or triple layer periodicity.

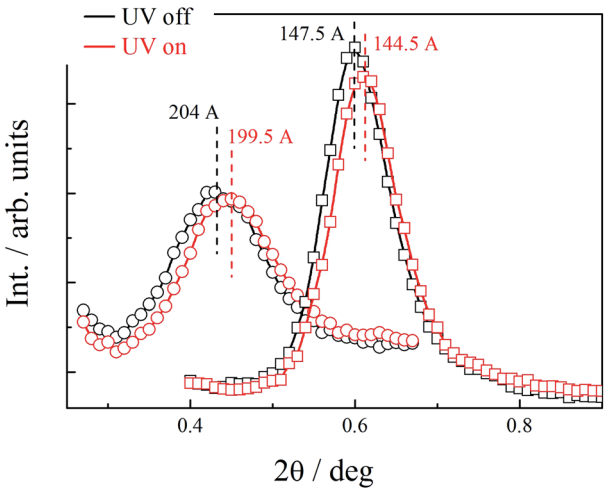

Fig. 4 Lowest angle XRD signals corresponding to basic periodicity in bilayer (squares) and triple-layer (circles) structures formed by annealed H5 material. Under UV illumination reversible shrinkage of the layers was observed.

temperature strongly depends on the organic shell composition, it is ~120 °C for the H1–H3 materials, while significantly higher, ~200 °C, for materials H4 and H5 containing ligands with fluorinated chain.

Owing to the presence of photosensitive azo unit in the ligand L1–L3 molecules the structure formed by hybrid nanoparticles can be tuned with a UV light through *trans–cis* isomerization of N=N bond. For material H5 it was observed, that although irradiation of the sample did not disturb the general organization of NPs into lamellar structure, it resulted in shrinking of the layer thickness by ~3%, the changes were reversible, layer thickness increased to the initial value after switching-off the UV light. Interestingly, the influence of the UV irradiation was observed for both, bi- and triple-layer H5 structures (Fig. 4).

In conclusion, new type of Janus-type structures were obtained, their asymmetry is a result of functionalization of metal surface with two chemically incompatible mesogenic ligands: having alkyl and fluorinated terminal chains. The nanoparticles form lamellar structures in which ligands of the covering layer self-segregate. Either bilayer structure with separate sublayers of alkyl and fluorinated ligands if formed, or in case of rapid temperature annealing the triple-layer structure in which some sublayers with mixed composition of ligands remain. Presence of photosensitive azo units in the ligand molecules allowed for reversible shrinkage of the layers by UV irradiation, the effect was observed for both bilayer and triple-layer structures.

Conflicts of interest

There are no conflicts to declare.

Acknowledgements

The presented studies were supported by The National Science Centre, Poland, no. 2017/01/X/ST5/01863. M. T. acknowledges

support from Ministry of Science and Higher Education, funds for science 2019–2023, within Diamentowy grant project (0112/DIA/2019/48).

Notes and references

1 T. Hegmann, H. Qi and V. M. Marx, *J. Inorg. Organomet. Polym. Mater.*, 2007, **17**, 483.
2 S. Saliba, C. Mingotaud, M. L. Kahn and J.-D. Marty, *Nanoscale*, 2013, **5**, 6641.
3 W. Lewandowski, M. Fruhnert, J. Mieczkowski, C. Rockstuhl and E. Górecka, *Nat. Commun.*, 2015, **6**, 6590.
4 Z. Xue, C. Yan and T. Wang, *Adv. Funct. Mater.*, 2019, **29**, 1807658.
5 H. K. Bisoyi and S. Kumar, *Chem. Soc. Rev.*, 2011, **40**, 306.
6 C. N. R. Rao, G. U. Kulkarni, P. J. Thomas and P. P. Edwards, *Chem. Soc. Rev.*, 2000, **29**, 27.
7 A. L. Rogach, N. Gaponik, J. M. Lupton, C. Bertoni, D. E. Gallardo, S. Dunn, N. L. Pira, M. Paderi, P. Repetto, S. G. Romanov, C. O'Dwyer, C. M. Sotomayor Torres and A. Eychmüller, *Angew. Chem., Int. Ed.*, 2008, **47**, 6538.
8 G. Konstantatos, I. Howard, A. Fischer, S. Hoogland, J. Clifford, E. Klem, L. Levina and E. H. Sargent, *Nature*, 2006, **442**, 180.
9 G. L. Nealon, R. Greget, C. Dominguez, Z. T. Nagy, D. Guillon, J.-L. Gallaniand and B. Donnio, *Beilstein J. Org. Chem.*, 2012, **8**, 349.
10 M. Baginski, M. Tupikowska, G. González-Rubio, M. Wójcik and W. Lewandowski, *Adv. Mater.*, 2020, **32**, 1904581.
11 M. Sarikaya, C. Tamerler, A. K.-Y. Jen, K. Schulten and F. Baneyx, *Nat. Mater.*, 2003, **2**, 577.
12 J. Hu, S. Zhou, Y. Sun, X. Fang and L. Wu, *Chem. Soc. Rev.*, 2012, **41**, 4356.
13 F. Liang, C. Zhang and Z. Yang, *Adv. Mater.*, 2014, **26**, 6944.
14 A. Perro, S. Reculusa, S. Ravaine, E. Bourgeat-Lami and E. Duguet, *J. Mater. Chem.*, 2005, **15**, 3745.
15 X. Hou, S. Guan, T. Qu, X. Wu, D. Wang, A. Chen and Z. Yang, *ACS Macro Lett.*, 2018, **7**, 1475.
16 M. Ha, J.-H. Kim, M. You, Q. Li, C. Fan and J.-M. Nam, *Chem. Rev.*, 2019, **119**, 12208.
17 F. Tu and D. Lee, *J. Am. Chem. Soc.*, 2014, **136**, 9999.
18 Q. Chen, S. C. Bae and S. Granick, *Nature*, 2011, **469**, 381.
19 W. Gao, A. Pei, X. Feng, C. Hennessy and J. Wang, *J. Am. Chem. Soc.*, 2013, **135**, 998.
20 W. Li, H. Palis, R. Mérindol, J. Majimel, S. Ravaine and E. Duguet, *Chem. Soc. Rev.*, 2020, **49**, 1955.
21 A. Walther and A. H. E. Müller, *Chem. Rev.*, 2013, **113**(7), 5194.
22 X. Han, L. Wu, H. Zhang, A. He and H. Nie, *ACS Appl. Mater. Interfaces*, 2019, **11**(13), 12190.
23 D. Rodríguez-Fernández and L. M. Liz-Marzán, *Part. Part. Syst. Charact.*, 2013, **30**, 46.
24 C. Vilain, F. Goettmann, A. Moores, P. Le Floch and C. Sanchez, *J. Mater. Chem.*, 2007, **17**, 3509.
25 S. Pradhan, L. Xu and S. Chen, *Adv. Funct. Mater.*, 2007, **17**, 2385.
26 R. T. M. Jakobs, J. van Herrikhuyzen, J. C. Gielen, P. C. M. Christianen, S. C. J. Meskers and A. P. H. J. Schennin, *J. Mater. Chem.*, 2008, **18**, 3438.
27 B. Wang, B. Li, B. Zhao and C. Y. J. Li, *J. Am. Chem. Soc.*, 2008, **130**, 11594.
28 A. Prominski, E. Tomczyk, M. Pawlak, A. Jedrych, J. Mieczkowski, W. Lewandowski and M. Wójcik, *Materials*, 2020, **13**, 875.
29 A. M. Percebom, J. J. Giner-Casares, N. Claes, S. Bals, W. Loh and L. M. Liz-Marzán, *Chem. Commun.*, 2016, **52**, 4278.
30 D. Li, Y. Luo, J. Lan, Z. Luo, F. Li and K. Luo, *Gold Bull.*, 2020, **53**, 55.
31 K. C. Elbert, D. Jishkariani, Y. Wu, J. D. Lee, B. Donnio and C. B. Murray, *Chem. Mater.*, 2017, **29**(20), 8737.
32 E. R. Zubarev, J. Xu, A. Sayyad and J. D. Gibson, *J. Am. Chem. Soc.*, 2006, **128**, 4958–4959.
33 J. M. Wolska, D. Pociecha, J. Mieczkowski and E. Gorecka, *Chem. Commun.*, 2014, **50**, 7975.
34 J. M. Wolska, D. Pociecha, J. Mieczkowski and E. Gorecka, *Soft Matter*, 2013, **9**, 3005.
35 M. Brust, M. Walker, D. Bethell, D. J. Schiffrin and R. Whyman, *J. Chem. Soc., Chem. Commun.*, 1994, 801.
36 W. Lewandowski, K. Jatczak, D. Pociecha and J. Mieczkowski, *Langmuir*, 2013, **29**, 3404.
37 M. Wojcik, W. Lewandowski, J. Matraszek, J. Mieczkowski, J. Borysiuk, D. Pociecha and E. Gorecka, *Angew. Chem., Int. Ed.*, 2009, **48**, 5167.
38 M. Wojcik, M. Kolpaczynska, D. Pociecha, J. Mieczkowski and E. Gorecka, *Soft Matter*, 2010, **6**, 5397.